

Supporting Information for:

Toward Reliable Algorithmic Self-Assembly of DNA Tiles: A Fixed-Width Cellular Automaton Pattern

Kenichi Fujibayashi,[†] Rizal Hariadi,[‡] Sung Ha Park,[§] Erik Winfree,^{||,⊥} and Satoshi Murata^{*,†}

[†] Department of Computational Intelligence and Systems Science, Tokyo Institute of Technology, Midori-ku, Yokohama 226-8502, Japan

[‡] Department of Applied Physics, California Institute of Technology, Pasadena, CA 91125, USA

[§] Center for the Physics of Information, California Institute of Technology, Pasadena, CA 91125, USA

^{||} Department of Computation and Neural Systems, California Institute of Technology, Pasadena, CA 91125, USA

[⊥] Department of Computer Science, California Institute of Technology, Pasadena, CA 91125, USA

* E-mail: murata@dis.titech.ac.jp

Notes

Nucleation

Since in the range of conditions we are considering, tile attachment by a single sticky end is thermodynamically unfavorable, while attachment by two sticky end bonds is favorable, there is a kinetic barrier to the formation of assemblies if all possible assembly paths involve multiple unfavorable tile attachment steps. The critical nucleus for spontaneous growth of a thermodynamically favorable structure, such as a DNA tile ribbon, is (roughly) the supramolecular assembly requiring the fewest unfavorable attachments that nonetheless can grow into the full structure by means of subsequent exclusively favorable attachments. This principle was used to design ribbons with significant nucleation barriers [1], which allowed excellent control over nucleation with origami seeds (R. D. Barish, personal communication). In this work, the boundary tiles were intended create a barrier to nucleation requiring 4 unfavorable attachments to form a critical nucleus, but upon re-examination we realized that alternative tile arrangements produced a variety of ribbons with smaller nucleation barriers (see Figure S12). Thus, we expect that a redesigned tile set could reduce spurious nucleation further.

Lattice defects

A total of 22 ribbons were imaged at high resolution. Eight of these ribbons had widths thinner than designed, apparently due to lattice defect errors in the initial row. These eight were not analyzed; only the remaining fourteen were interpreted tile-by-tile for estimating growth errors. The frequency of lattice defect errors in the initial row could be due to the space between the double helices in the DNA origami being slightly narrower than that of the lattice made of DX molecules, which can be seen from the swelling that occurs between the origami seed and the fully grown ribbon crystal. In images that did not provide clear single-tile resolution, it was not possible to definitively detect lattice defects. All definitive lattice defects decreased the width of ribbons; we have no explanation for this observation. In the 14 analyzed ribbons, no lattice defect errors were observed within the first 15 rows, suggesting that during early ribbon growth (prior to stoichiometric disproportionation of tiles) the lattice defect rate may have been as low as 0.02% per tile. This contrasts dramatically with algorithmic crystals grown from floppy single-stranded nucleating strands [2, 3], where lattice defect rates were comparable to growth error rates. In that work it was suggested that multiple crystals nucleated independently at several locations along each nucleating strand, and lattice defects arose as these microcrystals subsequently merged with imperfect geometric alignment. Thus, the rigidity of the origami seed appears to help prevent this mode of lattice defect generation.

Methods

DNA sequences

All sequences are written 5' to 3'.

The universal strut strand

OTMU (16-mer) - GCTTGACACCAGAACG

Putting the sticky ends on the long strands makes it unlikely that malformed tiles lack either input or output or that the sticky ends could dissociate from the tiles. Furthermore, the short strands no longer need to carry tile-type-specific information, thus making the universal strand possible. Advantages of the universal strand design are that each new tile requires only two new strands, reducing synthesis effort, and that this makes proper stoichiometry easier to achieve – especially since the universal strand can be provided at in excess without ill consequences. Note that due to DNA strand polarity, these tiles attach with alternating orientation in each layer (see Figure S2).

XOR tiles (OTM00, OTM11, OTM01 and OTM10)

OTM00.1 (58-mer) - GAGATCGTTCTGGACCGCACCGATGTTACCTTAGAGCGTAGACCTGTCAAGCAGTGA
OTM00.2 (58-mer) - ATCTCCGTTCTGGTGAACATCGGTGCGGTGGTCTACGCTCTAAGGTGTCAAGCTCACT
OTM11.1 (58-mer) - TCTTGCGTTCTGGACTCTCGGCTAATCCACCTACAACCGACTACCTGTCAAGCGTATG
OTM11.2 (58-mer) - ATCTCCGTTCTGGTGGATTAGCCGAGAGTGGTAGTCGGTTGTAGGTGTCAAGCTCACT
OTM01.1 (58-mer) - TCTTGCGTTCTGGACTTGCAGCCAAATCACCTTAGGTCGCTACCTGTCAAGCAGTGA
OTM01.2 (102-mer) - CAAGACGTTCTGGTGATTTGGTGCCGTCGTTTTTCGACGGCATTCTGCAAGTGGTAGCGAC
TCGGATGTTTTTCATCCGAGTTCCTAAAGGTGTCAAGCCATAC
OTM10.1 (58-mer) - GAGATCGTTCTGGACTTTCGACAGACATTCACCTATTTGGACTCGCCTGTCAAGCGTATG
OTM10.2 (102-mer) - CAAGACGTTCTGGTGAATGTGTCGTCATCGTTTTTCGATGGACTTTCGCAAGTGGCGAGTGT
CCGCAGCTTTTGTGCGGATTCCAATAGGTGTCAAGCCATAC

32 adapters (seed for patterned cone-growth experiments)

OTMAdp1 (24-mer) - CGTTCTGGTGAAAAGTATTAAGAGG
OTMAdp2 (29-mer) - CTATTATTCTGAAACATGTCAAGCTCACT
OTMAdp3 (29-mer) - ATCTCCGTTCTGGGTCAGACGATTGGCCT
OTMAdp4 (29-mer) - CAGGAGGTTGAGGCAGTGTCAAGCTCACT
OTMAdp5 (29-mer) - ATCTCCGTTCTGGGCGTCAGACTGTAGCG
OTMAdp6 (29-mer) - ATCAAGTTTGCCTTTATGTCAAGCTCACT
OTMAdp7 (29-mer) - ATCTCCGTTCTGGAGACAAAAGGGCGACA
OTMAdp8 (29-mer) - GGTTTACCAGCGCCAATGTCAAGCTCACT
OTMAdp9 (29-mer) - ATCTCCGTTCTGGGCAGATAGCCGAACAA
OTMAdp10 (29-mer) - TTTTAAAGAAAAGTAATGTCAAGCTCACT
OTMAdp11 (29-mer) - ATCTCCGTTCTGGAACGTCAAAAATGAAA
OTMAdp12 (29-mer) - AAACGATTTTTTGTGTTTGTCAAGCTCACT
OTMAdp13 (29-mer) - ATCTCCGTTCTGGGCTTATCCGGTATTCT
OTMAdp14 (29-mer) - AAATCAGATATAGAAGTGTCAAGCTCACT
OTMAdp15 (29-mer) - ATCTCCGTTCTGGACGCGCCTGTTTATCA
OTMAdp16 (29-mer) - GTTCAGCTAATGCAGATGTCAAGCTCACT
OTMAdp17 (29-mer) - CAAGACGTTCTGGGAAAAAGCCTGTTTAG
OTMAdp18 (29-mer) - GGAATCATAATTACTATGTCAAGCTCACT
OTMAdp19 (29-mer) - ATCTCCGTTCTGGCATAGGTCTGAGAGAC
OTMAdp20 (29-mer) - GTGAATTTATCAAATTTGTCAAGCTCACT
OTMAdp21 (29-mer) - ATCTCCGTTCTGGGAAGATGATGAAACAA
OTMAdp22 (29-mer) - AATTACCTGAGCAAAATGTCAAGCTCACT
OTMAdp23 (29-mer) - ATCTCCGTTCTGGACTTCTGAATAATGGA
OTMAdp24 (29-mer) - TGATTGTTTGGATTATTGTCAAGCTCACT

OTMAdp25 (29-mer) - ATCTCCGTTCTGGGCCGTCAATAGATAAT
 OTMAdp26 (29-mer) - CAACTAATAGATTAGATGTCAAGCTCACT
 OTMAdp27 (29-mer) - ATCTCCGTTCTGGCCAGCAGAAGATAAAA
 OTMAdp28 (29-mer) - AATACCGAACGAACCATGTCAAGCTCACT
 OTMAdp29 (29-mer) - ATCTCCGTTCTGGCTACATTTTGACGCTC
 OTMAdp30 (29-mer) - ACGCTCATGGAAATACTGTCAAGCTCACT
 OTMAdp31 (29-mer) - ATCTCCGTTCTGGCAGGAACGGTACGCCA
 OTMAdp32 (24-mer) - TTAAGGGATTTTAGATGTCAAGC

Boundary single tiles (sT0, sT1, sT2, sT3)

sT0.1 (58-mer) - AACCTCGTTCTGGACGCTGTGGCTATTACCTCTAACTCCGATCCTGTCAAGCAGTGA
 sT0.2 (58-mer) - AGGTTCTGTTCTGGTGAATAGCCACAGCGTGGATCGGAGTTAGAGGTGTCAAGCTCACT
 sT1.1 (58-mer) - AACCTCGTTCTGGACTGCGTCTGATCTCACCGTTTGCCTGCATCCTGTCAAGCGTATG
 sT1.2 (58-mer) - AGGTTCTGTTCTGGTGAATAGCCACAGCGTGGATCGGAGTTAGAGGTGTCAAGCTCACT
 sT2.1 (58-mer) - GAGATCGTTCTGGACTGCCACGACTATCACCTTTGCTCATCGACCTGTCAAGCGGTAA
 sT2.2 (58-mer) - ATCTCCGTTCTGGTGAATAGCTCGTGGCAGTGGTTCGATGAGCAAAGGTGTCAAGCTTACC
 sT3.1 (58-mer) - TCTTTCGTTCTGGACTAGGAGCATTAGCACCTTCATCAGCGGACCTGTCAAGCGGTAA
 sT3.2 (58-mer) - CAAGACGTTCTGGTGAATAGCTCGTGGTCCGCTGATGAAGGTGTCAAGCTTACC

Boundary double tiles (dT0, dT1)

dT0.1 (58-mer) - AACCTCGTTCTGGACGCTCAACTGTATCACCTTATCCGAAGATCCTGTCAAGCTTAGC
 dT0.2 (92-mer) - AGGTTCTCATTGGTGATACAGTTGAGCGTGGATCTTCGGATAAGGTGTTTACCGAGTAGG
 CTTCCACCGTCTCGATCACCTTTTGGGTGAT
 dT0.3 (69-mer) - CGAGACGGACTCTGCTCCATTTACCTAACAGCTACGACCTGGAAGCCTACTCGGTAAACACCAATGAG
 dT0.4 (71-mer) - GACATCCTTTTGGATGTCCGTTCTGGTGAATGGAGCAGAGTGGTTCGATGCTGTTAGGTGTCAAGCGCTAA
 dT1.1 (58-mer) - ACAAGCGTTCTGGACTGACGCCTCAATCACCTATAACCACAGACCTGTCAAGCGGTAA
 dT1.2 (74-mer) - GTTGTCCACCTGCGATAGGCAGATTACGGTGAATTGAGGCGTCAGTGGCTCTGTGGTATAGGTGCAATTCTTACC
 dT1.3 (87-mer) - GAATTGCACCGTAATCTGCCTATCGCAGGACTCACGGATACTTCACCTTGTTCGCCAAAC
 CTGGACAACCCATTCTTTTGGAAATGG
 dT1.4 (71-mer) - CTTGTCTGTTCTGGTGAAGTATCCGTGAGTGGTGGCGAAACAAGGTGTCAAGCACTCACCTTTTGGTGAGT

32 adapters (seed for patterned ribbon-growth experiments)

OTMAdp1 (24-mer) - CGTTCGGTGAAGTATTAAGAGG
 OTMAdp2-s2 (29-mer) - CTATTATCTGAAACATGTCAAGCGCTAA
 OTMAdp3-s3 (29-mer) - AGGTTCTGTTCTGGGTGACGATTGGCCT
 OTMAdp4-s1 (29-mer) - CAGGAGGTTGAGGCAGTGTCAAGCCATAC
 OTMAdp5-s1 (29-mer) - CAAGACGTTCTGGGCGTCAGACTGTAGCG
 OTMAdp6-s1 (29-mer) - ATCAAGTTTGCCTTTATGTCAAGCCATAC
 OTMAdp7 (29-mer) - ATCTCCGTTCTGGAGACAAAAGGGCGACA
 OTMAdp8 (29-mer) - GGTTTACCAGCGCCAATGTCAAGCTCACT
 OTMAdp9 (29-mer) - ATCTCCGTTCTGGGAGATAGCCGAACAA
 OTMAdp10 (29-mer) - TTTTAAAGAAAAGTAATGTCAAGCTCACT
 OTMAdp11-s1 (29-mer) - CAAGACGTTCTGGAACGTCAAAAATGAAA
 OTMAdp12-s1 (29-mer) - AAACGATTTTTTGTGTTTGTCAAGCCATAC
 OTMAdp13-s1 (29-mer) - CAAGACGTTCTGGGCTTATCCGGTATTCT
 OTMAdp14-s1 (29-mer) - AAATCAGATATAGAAGTGTCAAGCCATAC
 OTMAdp15 (29-mer) - ATCTCCGTTCTGGACGCGCCTGTTTATCA
 OTMAdp16 (29-mer) - GTTCAGCTAATGCAGATGTCAAGCTCACT
 OTMAdp17-s0 (29-mer) - ATCTCCGTTCTGGGAAAAGCCTGTTTAG
 OTMAdp18 (29-mer) - GGAATCATAATTACTATGTCAAGCTCACT
 OTMAdp19-s1 (29-mer) - CAAGACGTTCTGGCATAGGTCTGAGAGAC
 OTMAdp20-s1 (29-mer) - GTGAATTTATCAAAAATGTCAAGCCATAC

OTMAdp21-s1 (29-mer) - CAAGACGTTCTGGGAAGATGATGAAACAA
OTMAdp22-s1 (29-mer) - AATTACCTGAGCAAAATGTCAAGCCATAC
OTMAdp23 (29-mer) - ATCTCCGTTCTGGACTTCTGAATAATGGA
OTMAdp24 (29-mer) - TGATTGTTTGGATTATTGTCAAGCTCACT
OTMAdp25 (29-mer) - ATCTCCGTTCTGGGCCGTCAATAGATAAT
OTMAdp26 (29-mer) - CAACTAATAGATTAGATGTCAAGCTCACT
OTMAdp27-s1 (29-mer) - CAAGACGTTCTGGCCAGCAGAAGATAAAA
OTMAdp28-s1 (29-mer) - AATACCGAACGAACCATGTCAAGCCATAC
OTMAdp29-s1 (29-mer) - CAAGACGTTCTGGCTACATTTGACGCTC
OTMAdp30-s4 (29-mer) - ACGCTCATGGAAATACTGTCAAGCTTACC
OTMAdp31-s5 (29-mer) - CTTGTCGTTCTGGCAGGAACGGTACGCCA
OTMAdp32 (24-mer) - TTAAAGGGATTTTAGATGTCAAGC

Figures

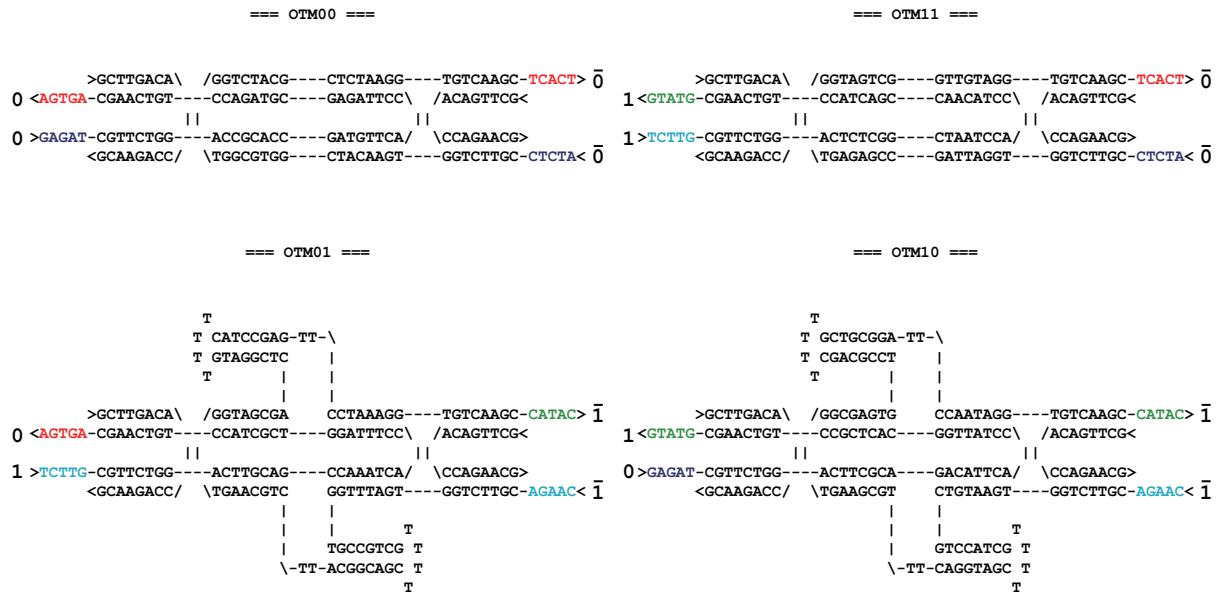


Figure S1: Diagrams of XOR tiles. The distance between crossover points is 16-bp. The 22-nt hairpins on '1' tiles are positioned symmetrically, so that the topographical contrast for AFM is centered, and the same in either tile orientation.

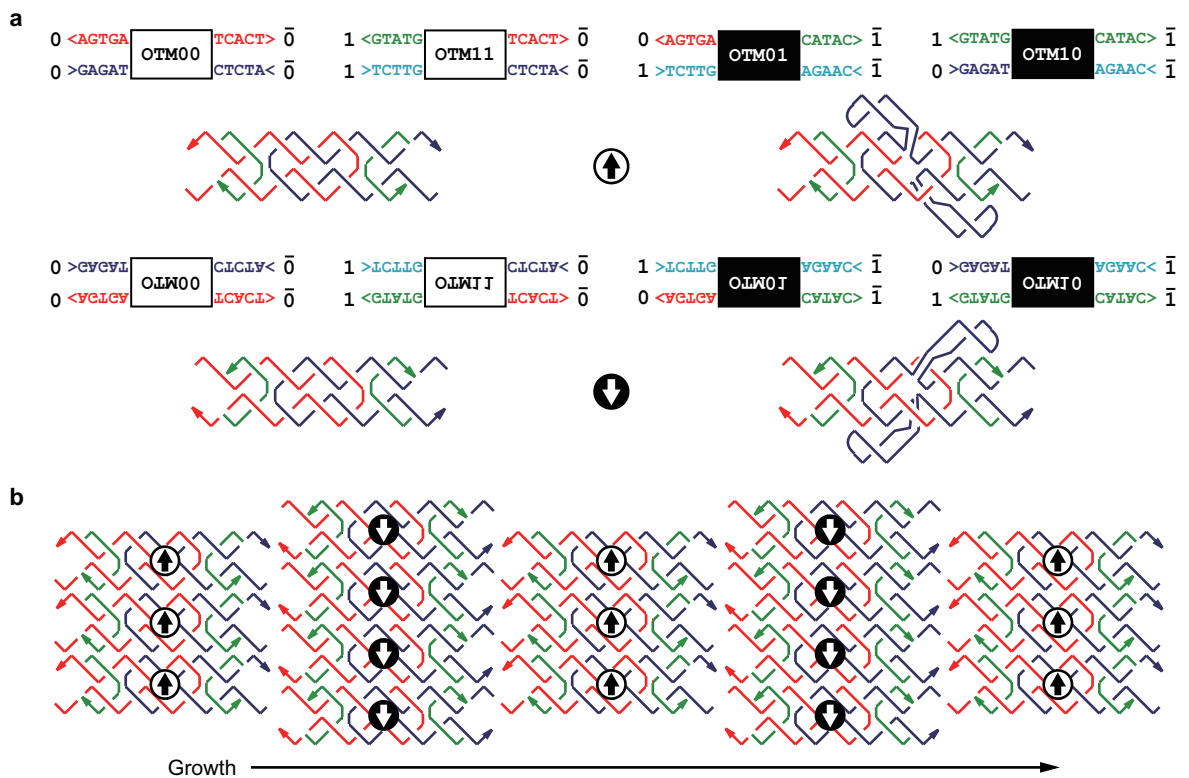


Figure S2: Lattice assembly by XOR tiles. (a) The four XOR tiles (top) and the same tiles flipped horizontally (bottom). OTM01 and OTM10 tiles have one hairpin per helix. (b) Growth of tiles. Properly seeded crystals grow to the right. Tiles bind in a flipped orientation on alternate rows. For cellular automata growth rules that are not symmetric, this tile design would require distinct tiles for alternate rows, doubling the size of the tile set.

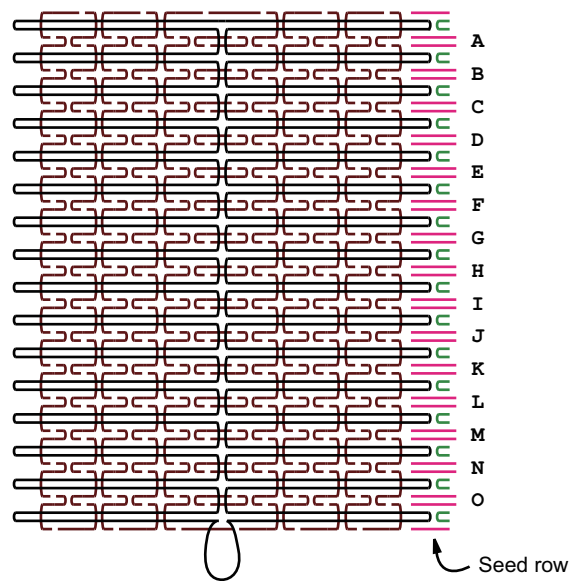


Figure S3: Rectangular DNA origami with adapter strands and universal strands (origami seed). The origami is composed of 7249-nt M13mp18 single strand (black) and 192 different staple strands (brown). 32 different adapter strands (magenta) and sixteen copies of the universal strut strand (green) bind to form the right side of the origami seed. Thus, the right side of the origami seed conforms exactly to the modified DX motif used for the rule tiles, except that there is a nick at the crossover point, resulting in magenta strands that are shorter than the analogous strands in the DX motif. This reduces the potential for binding between the green and magenta strands prior to attachment to the seed, and also allows us to forgo purification of the magenta strands because they are shorter. The left side of the origami has unstructured single-stranded loops to prevent stacking of origami.

.....>CCTCTTAATACTTTCA\ /CCAGAACG> <GGAGAATTTATGAAAGT---GGTCTTGC<	OTMAdp1>CTAAACAGGCTTTTTC\ /CCAGAACG> <GATTTGTCCGAAAAAG---GGTCTTGC-AGAAC<	OTMAdp17
 >CTATTTATCTGAAACA---TGTCAAGC- TCACT >	OTMAdp2	 >GGAATCATAAATTAATA---TGTCAAGC- TCACT >	OTMAdp18
.....<GATAATAAGACTTTGT/ \ACAGTTCG<	<CCTTAGTATTATATGAT/ \ACAGTTCG<	
.....>AGGCCAATCGTGTGAC\ /CCAGAACG> <TCCGGTTAGCAGACTG---GGTCTTGC-CTCTA<	OTMAdp3>GTCTCTCAGACCTATG\ /CCAGAACG> <CAGAGAGTCTGGATAAC---GGTCTTGC-CTCTA<	OTMAdp19
 >CAGGAGGTTGAGGCAG---TGTCAAGC- TCACT >	OTMAdp4	 >GTGAATTTATCAAAAT---TGTCAAGC- TCACT >	OTMAdp20
.....<GTCTCCAACCTCCGTC/ \ACAGTTCG<	<CACTTAAATAGTTTAA/ \ACAGTTCG<	
.....>CGTACAGTCTGACGC\ /CCAGAACG> <GCGATGTCAAGACTGCG---GGTCTTGC-CTCTA<	OTMAdp5>TTGTTTCATCATCTTC\ /CCAGAACG> <AACAAAGTAGTAGAAG---GGTCTTGC-CTCTA<	OTMAdp21
 >ATCAAGTTTGCCTTTA---TGTCAAGC- TCACT >	OTMAdp6	 >AATTACCTGAGCAAAA---TGTCAAGC- TCACT >	OTMAdp22
.....<TAGTTCAAACGGAAAT/ \ACAGTTCG<	<TTAATGGACTCGTTTT/ \ACAGTTCG<	
.....>TGTGCGCCCTTTGTCT\ /CCAGAACG> <ACAGCGGGAAACAGAG---GGTCTTGC-CTCTA<	OTMAdp7>TCCATTATTCAGAAGT\ /CCAGAACG> <AGGTAATAAGTCTTCA---GGTCTTGC-CTCTA<	OTMAdp23
 >GGTTTACCAGCGCCAA---TGTCAAGC- TCACT >	OTMAdp8	 >TGATTGTTGGATTAT---TGTCAAGC- TCACT >	OTMAdp24
.....<CCAAATGGTCCGGTT/ \ACAGTTCG<	<ACTAACAAACCTAATA/ \ACAGTTCG<	
.....>TTGTTCCGGTATCTGC\ /CCAGAACG> <AACAAAGCCATAGACG---GGTCTTGC-CTCTA<	OTMAdp9>ATTATCTATTGACGGC\ /CCAGAACG> <TAATAGATAACTGCCG---GGTCTTGC-CTCTA<	OTMAdp25
 >TTTTTAAGAAAAGTAA---TGTCAAGC- TCACT >	OTMAdp10	 >CAACTAATAGATTAGA---TGTCAAGC- TCACT >	OTMAdp26
.....<AAAAATCTTTTCATT/ \ACAGTTCG<	<GTTGATTATCTAATCT/ \ACAGTTCG<	
.....>TTTCATTTTTCAGCTT\ /CCAGAACG> <AAAGTAAAAACTGCAA---GGTCTTGC-CTCTA<	OTMAdp11>TTTTATCTTCTGCTGG\ /CCAGAACG> <AAAAATAGAAGACGACC---GGTCTTGC-CTCTA<	OTMAdp27
 >AAACGATTTTTTGT---TGTCAAGC- TCACT >	OTMAdp12	 >AATACCGAACGAACCA---TGTCAAGC- TCACT >	OTMAdp28
.....<TTTGCTAAAAACAAA/ \ACAGTTCG<	<TTATGGCTTGCTTGGT/ \ACAGTTCG<	
.....>AGAATACCGGATAAGC\ /CCAGAACG> <TCTTATGGCTATTTCG---GGTCTTGC-CTCTA<	OTMAdp13>GAGCGTCAAAATGTAG\ /CCAGAACG> <CTCGCAGTTTTACATC---GGTCTTGC-CTCTA<	OTMAdp29
 >AAATCAGATATAGAAG---TGTCAAGC- TCACT >	OTMAdp14	 >ACGCTCATGGAATAC---TGTCAAGC- TCACT >	OTMAdp30
.....<TTTAGTCTATATCTTC/ \ACAGTTCG<	<TGCAGTACCTTTATG/ \ACAGTTCG<	
.....>TGATAAACAGGCGGT\ /CCAGAACG> <ACTATTTGTCCGCGCA---GGTCTTGC-CTCTA<	OTMAdp15>TGGCGTACCGTTCCTG\ /CCAGAACG> <ACCGCATGGCAAGGAC---GGTCTTGC-CTCTA<	OTMAdp31
 >GTTCAAGCTAATGCAGA---TGTCAAGC- TCACT >	OTMAdp16	 >TTAAAGGATTTTAGA---TGTCAAGC- TCACT >	OTMAdp32
.....<CAAGTCGATTACGCT/ \ACAGTTCG<	<AATTTCCCTAAAATCT/ \ACAGTTCG<	

Figure S4: Diagrams of 15 binding sites (A to O) for patterned cone-growth experiments. For all-'0' seeds, the sticky end on OTMAdp17 is replaced by ATCTC (5' to 3').

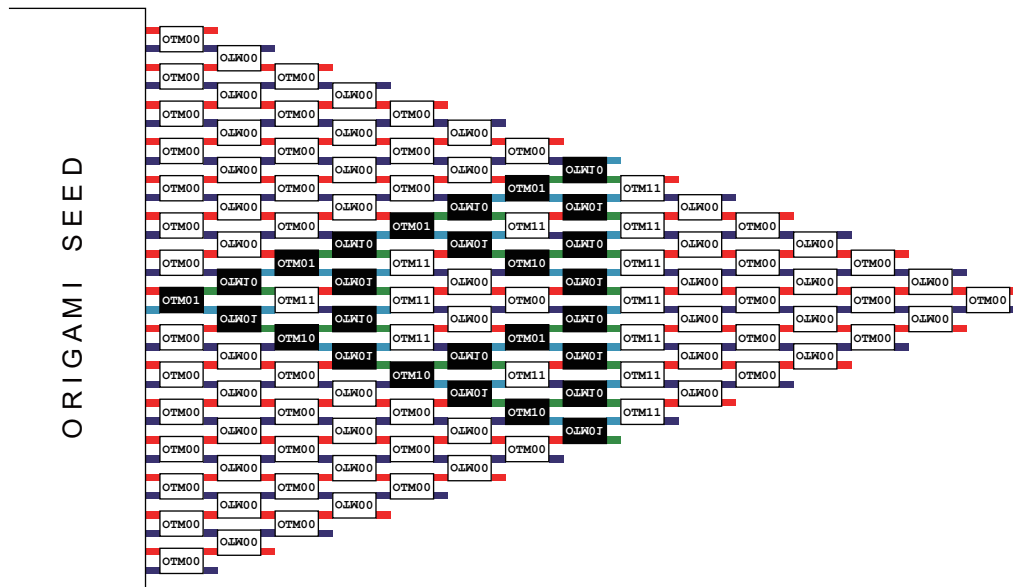


Figure S5: Design of the cone. Assembly from the seed by legal attachments (where each tile attaches by two matching sticky ends) results in the assembly shown, which contains 80 OTM00, 13 OTM11, 14 OTM01 and 13 OTM10 tiles. No further legal attachments may occur, since any single tile to be added must attach by a single sticky end.

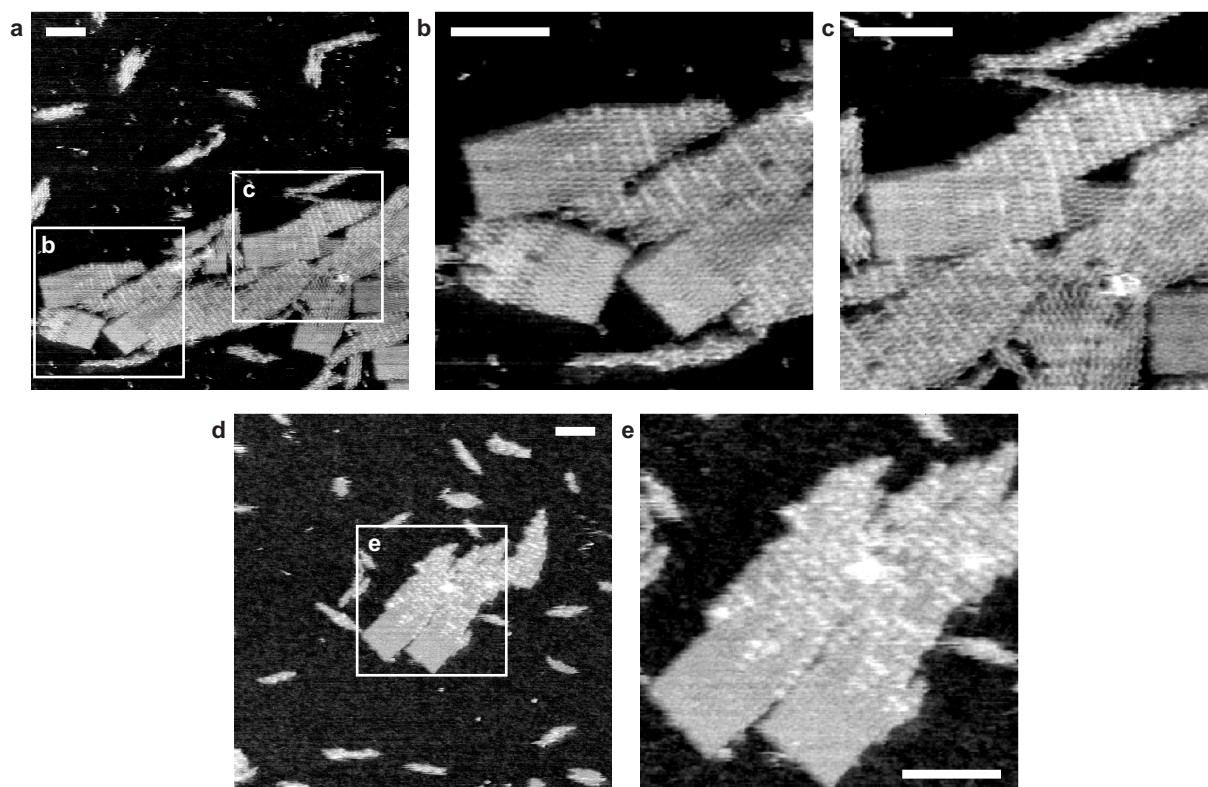


Figure S6: AFM images of cones (with patterns) grown using all XOR tiles. Significant amounts of facet nucleation and assembly merging can be seen. (a–c) [origami] = 1 nM, [OTM00] = [OTM11] = [OTM10] = 25 nM, [OTM01] = 125 nM. (d,e) [origami] = 1 nM, [OTM00] = [OTM11] = [OTM10] = 25 nM, [OTM01] = 250 nM. Scale bars are 100 nm.

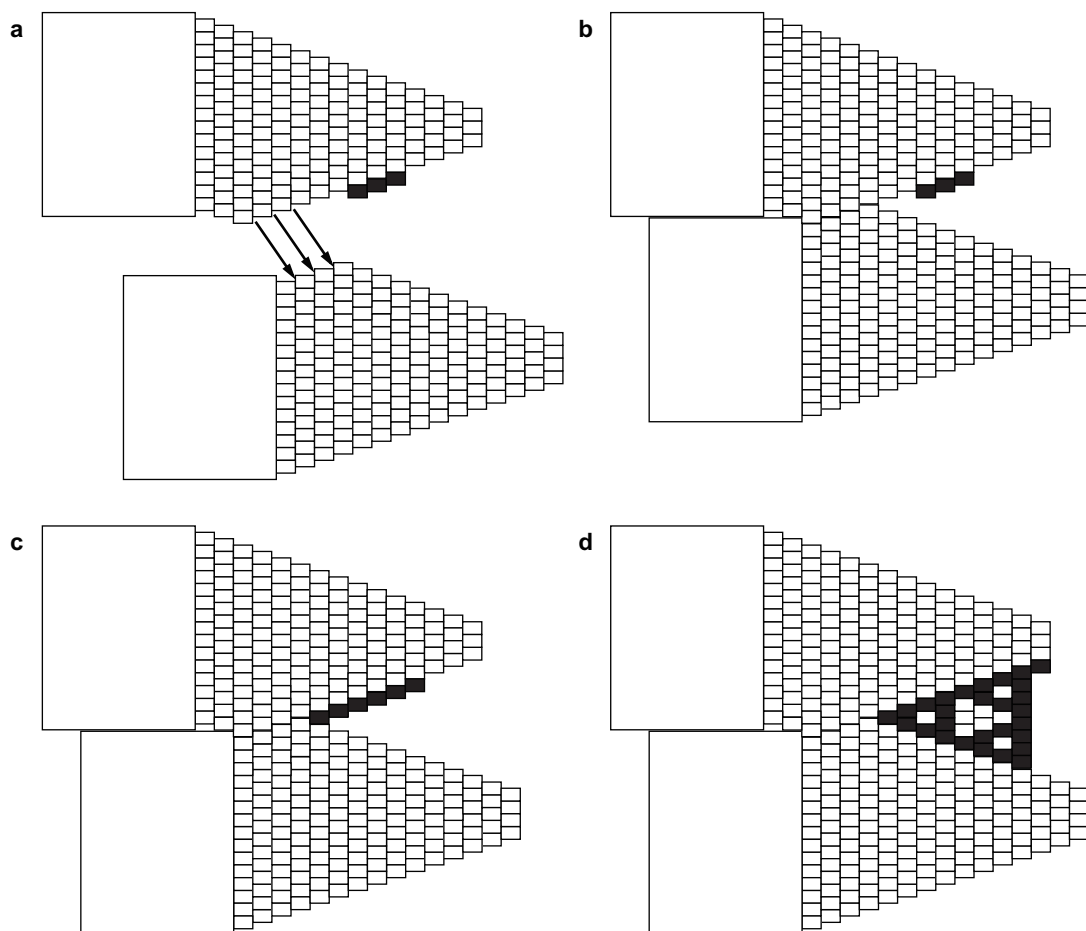


Figure S7: Aggregation and merging of cone assemblies: hypothetical assembly pathway. (a) Two origami cones experience facet nucleation, creating sites where the cones can attach to each other via multiple sticky ends. (b) Additional facet nucleation may result in a layer of '1' tiles. (c) Backwards growth is terminated by the corner formed by attachment. (d) Forward growth, e.g. of a Sierpinski pattern, completes the merging of the crystals.

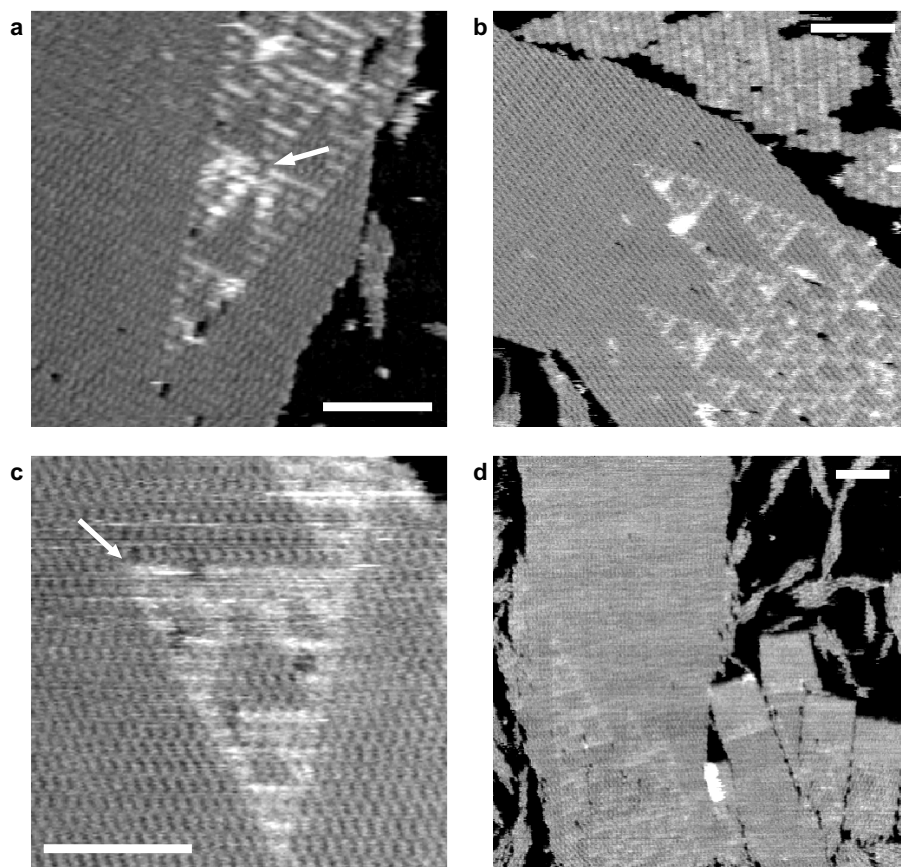


Figure S8: AFM images of large Sierpinski patterns observed in cone-growth experiments (a,b), and in ribbon-growth experiments (c,d). (a) is a magnified image of Figure 2e. In (a) and (b), [origami] = 1 nM, [each XOR tile] = 100 nM. In (c) and (d), [origami] = 1 nM, [each XOR tile] = 50 nM, [each boundary tile] = 10 nM. The white arrow in (a) indicates a deviation from the ideal Sierpinski pattern that appears to be due to a lattice defect error earlier in the assembly; the white arrow in (c) indicates the first growth error in that assembly. Many other errors are not identified. Scale bars are 100 nm.

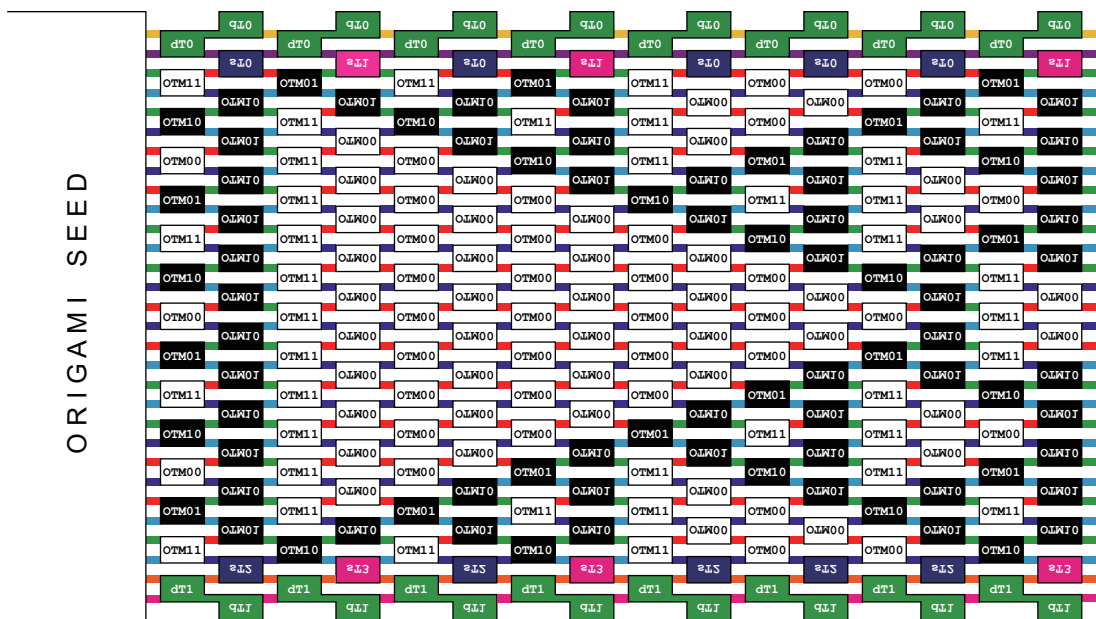


Figure S9: Design of the ribbon. Approximately one half of the period is shown. A full period contains 146 OTM00, 68 OTM11, 68 OTM01, 68 OTM10, 10 sT0 tiles, 4 sT1, 10 sT2, 4 sT3, 14 dT0 and 14 dT1 tiles. Ribbons that have grown just ten layers will have used 5 dT0, 5 dT1, 3 sT0, 2 sT1, 3 sT2, 2 sT3, 22 OTM01, 22 OTM10, 25 OTM11, and 56 OTM00. Thus, in a reaction where $[\text{origami}] = 1 \text{ nM}$ and $[\text{each XOR tile}] = 50 \text{ nM}$ and $[\text{each boundary tile}] = 10 \text{ nM}$, by the time most seeds have grown ten layers, the OTM00 tile will have been depleted but all other species will remain at significant concentrations.

```

=== sT0 ===
0 >GCTTGACA\ /GGATCGGA---GTTAGAG---TGTC AAGC-TCACT> 0̄
<AGTGA-CGAACTGT---CCTAGCCT---CAATCTCC\ /ACAGTTCG<
|| ||
>AACCT-CGTTCTGG---ACGCTGTG---GCTATTCA\ \CCAGAACG>
<GCAAGACC/ \TGC GACAC---CGATAAGT---GGTCTTGC-TTGA<

=== sT1 ===
1 >GCTTGACA\ /GGATGCAG---GCAAACGG---TGTC AAGC-CATAC> 1̄
<GTATG-CGAACTGT---CCTACGTC---CGTTTGCC\ /ACAGTTCG<
|| ||
>AACCT-CGTTCTGG---ACTGCGTC---GTATCTCA\ \CCAGAACG>
<GCAAGACC/ \TGACGCAG---CATAGAGT---GGTCTTGC-TTGA<

=== sT2 ===
0 >GCTTGACA\ /GGTCGATG---AGCAAAGG---TGTC AAGC-TTACC>
<AATGG-CGAACTGT---CCAGCTAC---TCGTTTCC\ /ACAGTTCG<
|| ||
>GAGAT-CGTTCTGG---ACTGCCAC---GACTATCA\ \CCAGAACG>
<GCAAGACC/ \TGACGGTG---CTGATAGT---GGTCTTGC-CTCTA< 0̄

=== sT3 ===
1 >GCTTGACA\ /GGTCCGCT---GATGAAGG---TGTC AAGC-TTACC>
<AATGG-CGAACTGT---CCAGGCGA---CTACTTCC\ /ACAGTTCG<
|| ||
>TCTTG-CGTTCTGG---ACTAGGAG---CATTAGCA\ \CCAGAACG>
<GCAAGACC/ \TGATCCTC---GTAATCGT---GGTCTTGC-AGAAC< 1̄

=== dT0 ===
/TT-CC-CACTA---GCTCTGCC\ /TGAGACGA---GGTAAAGT---GGTCTTGC---CTGTA-GG-TT\
\TT-GG-GTGAT> >CGAGACGG---ACTCTGCT---CCATTCCA\ /CCAGAACG> >GACAT-CC-TT\
|| ||
>GCTTGACA\ /GGATCTTC---GGATAAGG---TGTTTACC-GAGTA-\-CCGAAGGT---CCAGCATC---GACAATCC/ \ACAGTTCG<
<CGATG-CGAACTGT---CCTAGAAG---CCTATTCC\ /ACAAATGG-CTCAT-\-GGCTTCCA/ \GGTCGTAG---CTGTTAGG---TGTC AAGC-GCTAA>
|| ||
>AACCT-CGTTCTGG---ACGCTCAA---CTGTATCA\ \CCAATGAG>
<GCAAGACC/ \TGC GAGTT---GACATAGT---GGTTACTC-TTGA<

=== dT1 ===
>GCTTGACA\ /GGCTCTGT---GGTATAGG---TGCAATTC-TTACC>
<AATGG-CGAACTGT---CCGAGACA---CCATATCC\ /ACGTTAAG<
|| ||
>ACAAG-CGTTCTGG---ACTGACGC---CTCAATCA\ \CCGTAATC-TGCCT-\-TAGCGTCC\ /TGAGTGCC---TATGAAGT---GGTCTTGC-TGTTCC<
<GCAAGACC/ \TGACTGCG---GAGTTAGT---GGCATTAG-ACGGA-\-ATCGCAGG---ACTCACGG---ATACTTCA\ /CCAGAACG>
|| ||
/TT-CC-TTACC---CAACAGGT---CCAACCGC---TTTGTTC/ \ACAGTTCG< <TGAGT-GG-TT\
\TT-GG-AATGG> >GTTGTCCA/ \GGTTGGCG---AAACAAGG---TGTC AAGC---ACTCA-CC-TT\

```

Figure S10: Diagrams of single tiles (sT) and double tiles (dT).

.....>CCTCTTAATACTTTCA\ /CCAGAACG> <GGAGAATTATGAAAGT----GGTCTTGC<	OTMAdp1>CTAAACAGGCTTTTTC\ /CCAGAACG> <GATTTGTCCGAAAAAG----GGTCTTGC-CTCTA<	OTMAdp17-s0
 >CTATTATTCTGAAACA----TGTC AAGC-GCTAA><GATAATAAGACTTTGT/ \ACAGTTGC<	OTMAdp2-s2	 >GGAATCATAATTAATA----TGTC AAGC- TCACT ><CCTTAGTATAATGAT/ \ACAGTTGC<	OTMAdp18
.....>AGGCCAATCGTCTGAC\ /CCAGAACG> <TCCGGTTAGCAGACTG----GGTCTTGC-TTGA>	OTMAdp3-s3>GTCTCTCAGACCTATG\ /CCAGAACG> <CAGAGAGTCTGGATAC----GGTCTTGC- AGAAC <	OTMAdp19-s1
 >CAGGAGTTGAGGCAG----TGTC AAGC-CATAC><GTCCCTCAACTCCGTC/ \ACAGTTGC<	OTMAdp4-s1	 >GTGAATTTATCAAAAT----TGTC AAGC-CATAC><CACTTAAATAGTTTAA/ \ACAGTTGC<	OTMAdp20-s1
.....>CGTACAGTCTGACG\ /CCAGAACG> <GCGATGTCAGACTGCG----GGTCTTGC- AGAAC <	OTMAdp5-s1>TTGTTTCATCATCTTC\ /CCAGAACG> <AACAAAGTAGTAGAAG----GGTCTTGC- AGAAC <	OTMAdp21-s1
 >ATCAAGTTTGCCTTTA----TGTC AAGC-CATAC><TAGTTC A A A C G G A A A T / \ACAGTTGC<	OTMAdp6-s1	 >AATTACCTGAGCAAAA----TGTC AAGC-CATAC><TTAATGGACTCGTTTT/ \ACAGTTGC<	OTMAdp22-s1
.....>TGTGCGCCTTTGTCT\ /CCAGAACG> <ACAGCGGGAACAG----GGTCTTGC-CTCTA<	OTMAdp7>TCCATTATTCAGAAGT\ /CCAGAACG> <AGGTAATAAGTCTTCA----GGTCTTGC-CTCTA<	OTMAdp23
 >GGTTTACCAGCGCAA----TGTC AAGC- TCACT ><CCAATGGTCGCGGTT/ \ACAGTTGC<	OTMAdp8	 >TGATTGTTGGATTAT----TGTC AAGC- TCACT ><ACTAACAACCTAATA/ \ACAGTTGC<	OTMAdp24
.....>TTGTCGCTATCTGC\ /CCAGAACG> <AAACAGCGGATAGACG----GGTCTTGC-CTCTA<	OTMAdp9>ATTATCTATTGACGGC\ /CCAGAACG> <TAATAGATAACTGCCG----GGTCTTGC-CTCTA<	OTMAdp25
 >TTTTTAAGAAAAGTAA----TGTC AAGC- TCACT ><AAAAATTCCTTTTCAAT/ \ACAGTTGC<	OTMAdp10	 >CAACTAATAGATTAGA----TGTC AAGC- TCACT ><GTTGATTACTAATCT/ \ACAGTTGC<	OTMAdp26
.....>TTTCATTTTTCAGCTT\ /CCAGAACG> <AAAGTAAAAACTGCAA----GGTCTTGC- AGAAC <	OTMAdp11-s1>TTTTATCTTCTGCTGG\ /CCAGAACG> <AAAAATAGAAGACGACC----GGTCTTGC- AGAAC <	OTMAdp27-s1
 >AAACGATTTTGTGTT----TGTC AAGC-CATAC><TTTGCTAAAAACA AAA / \ACAGTTGC<	OTMAdp12-s1	 >AATACCGAACGAACCA----TGTC AAGC-CATAC><TTATGGCTTGCTTGGT/ \ACAGTTGC<	OTMAdp28-s1
.....>AGAATACCGGATAAGC\ /CCAGAACG> <TCTTATGGCCTATTTCG----GGTCTTGC- AGAAC <	OTMAdp13-s1>GAGCGTCAAAATGTAG\ /CCAGAACG> <CTCGAGTTTTACATC----GGTCTTGC- AGAAC <	OTMAdp29-s1
 >AAATCAGATATAGAAG----TGTC AAGC-CATAC><TTTAGTCTATATCTTC/ \ACAGTTGC<	OTMAdp14-s1	 >ACGCTCATGGAATAC----TGTC AAGC- TTACC ><TGGAGTACCTTTATG/ \ACAGTTGC<	OTMAdp30-s4
.....>TGATAACAGGCGCGT\ /CCAGAACG> <ACTATTTGTCGCGCA----GGTCTTGC-CTCTA<	OTMAdp15>TGCGTACCGTTCCTG\ /CCAGAACG> <ACCGCATGGCAAGGAC----GGTCTTGC- TGTTT <	OTMAdp31-s5
 >GTTCAAGTAAATGAGA----TGTC AAGC- TCACT ><CAAGTCGATTACGCT/ \ACAGTTGC<	OTMAdp16	 >TTAAAGGATTTTAGA----TGTC AAGC><AATTTCCCTAAAATCT/ \ACAGTTGC<	OTMAdp32

Figure S11: Diagrams of 15 binding sites (A to O) in seeds for the patterned ribbon-growth experiments. For all ‘0’ ribbons, the seed used adapter strands OTMAdp-s2, OTMAdp3-s3, OTMAdp30-s4, OTMAdp31-s5 as shown here, but in all other positions it used the same adapter strands as in the all-‘0’ cone-growth seed.

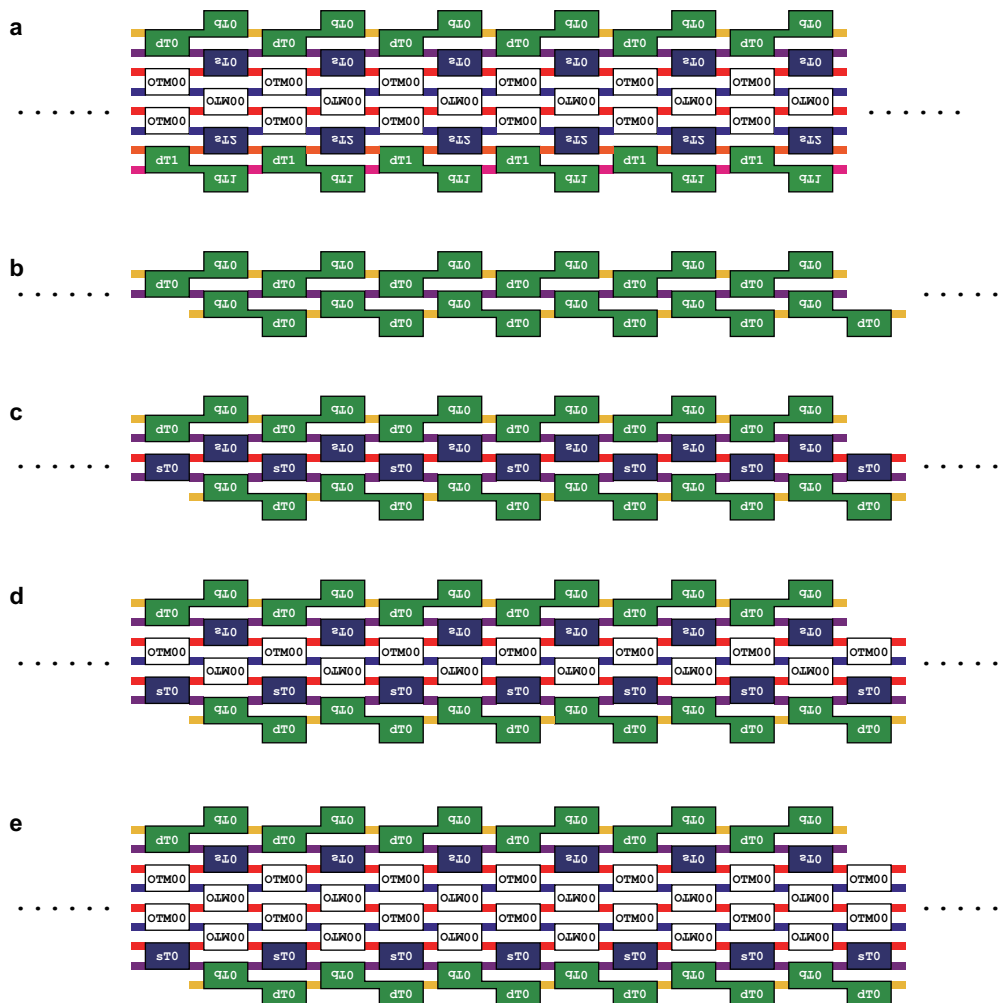


Figure S12: Examples of arbitrary-width ribbons that can grow without an origami seed if they nucleate. Such spuriously-nucleated ribbons must nucleate via a series of unfavorable tile attachments mediated by only a single sticky end; except at high tile concentrations and/or low temperatures, such tiles quickly dissociate. Thus the number of unfavorable attachments is a rough measure of the barrier to nucleation. (a) The smallest ribbon in which tiles are oriented analogously to the seed-nucleated ribbon. It contains OTM00, sT0, sT2, dt0, and dt1 tiles. Creating a critical nucleus requires 4 unfavorable attachments, which is expected to result in a significant kinetic barrier to spontaneous nucleation of this ribbon pattern. (b) A ribbon composed of only the dt0 tile, with a kinetic barrier of only a single unfavorable attachment. (c–e) Wider ribbons composed of OTM00, sT0 and dt0 tiles, requiring 3, 5, and 7 unfavorable attachments (respectively) to create a critical nucleus. Other widths can also form, as can patterned ribbons containing all the tile types. Note that a simple change of the sticky ends could prevent case (b) without disrupting the desired ribbon patterns, but preventing case (c) would require more tile types.

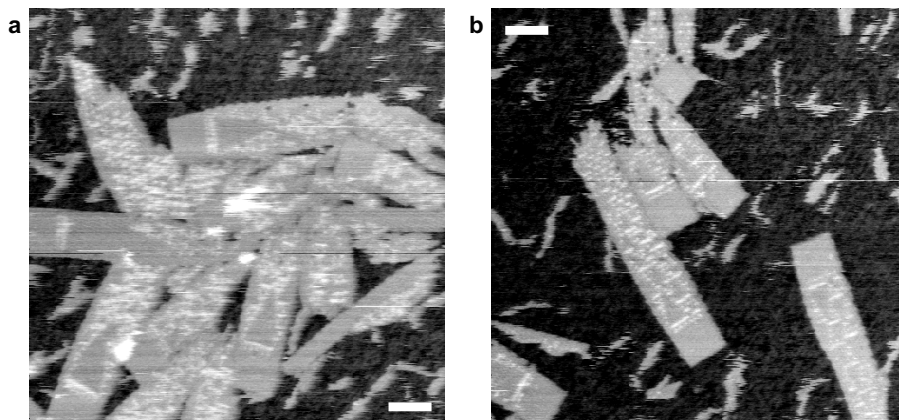


Figure S13: Typical AFM images of patterned ribbons grown using all XOR tiles. [origami] = 1 nM, [each XOR tile] = 50 nM, [each boundary tile] = 10 nM. Scale bars are 100 nm.

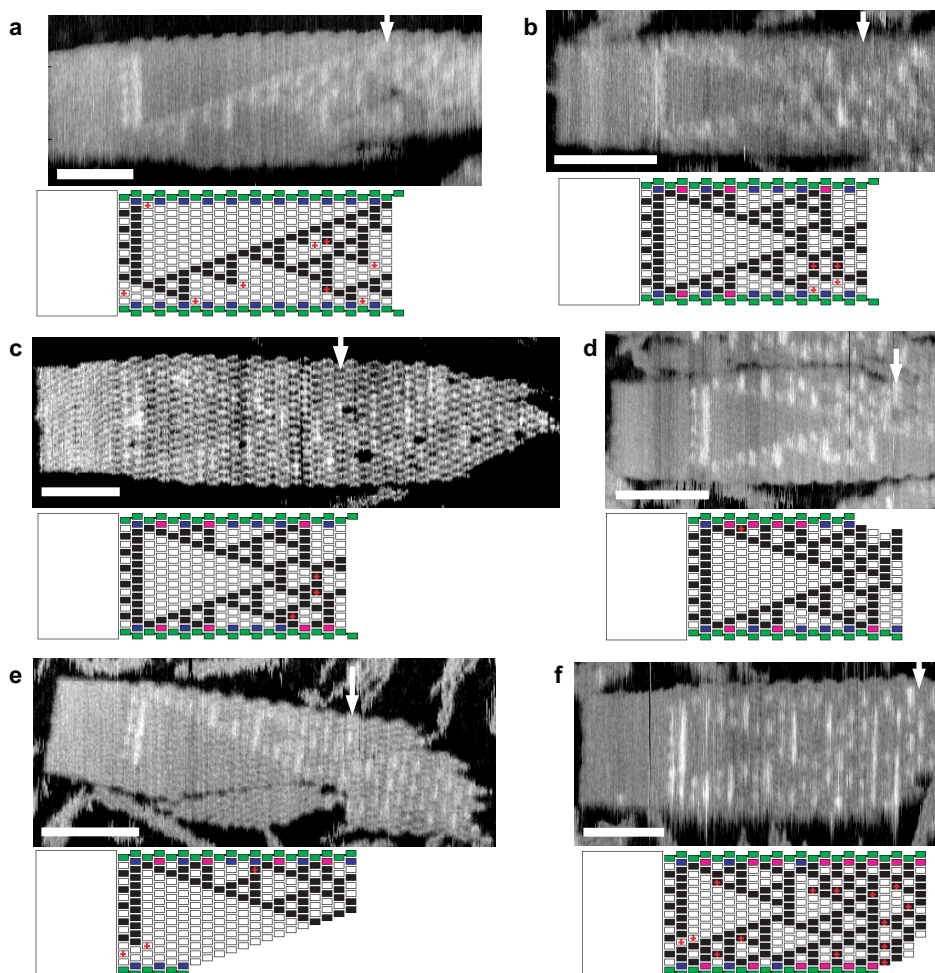


Figure S14: AFM images of six ribbons grown using all XOR tiles, and our interpretation of their tile patterns. There may be a lattice defect error in row 6 of (a), leading to a widening of the ribbon, but image quality is not high enough to say so definitively. A definitive lattice defect error can be seen in row 20 of (c). [origami] = 1 nM, [each XOR tile] = 50 nM, [each boundary tile] = 10 nM. Scale bars in the images are 100 nm.

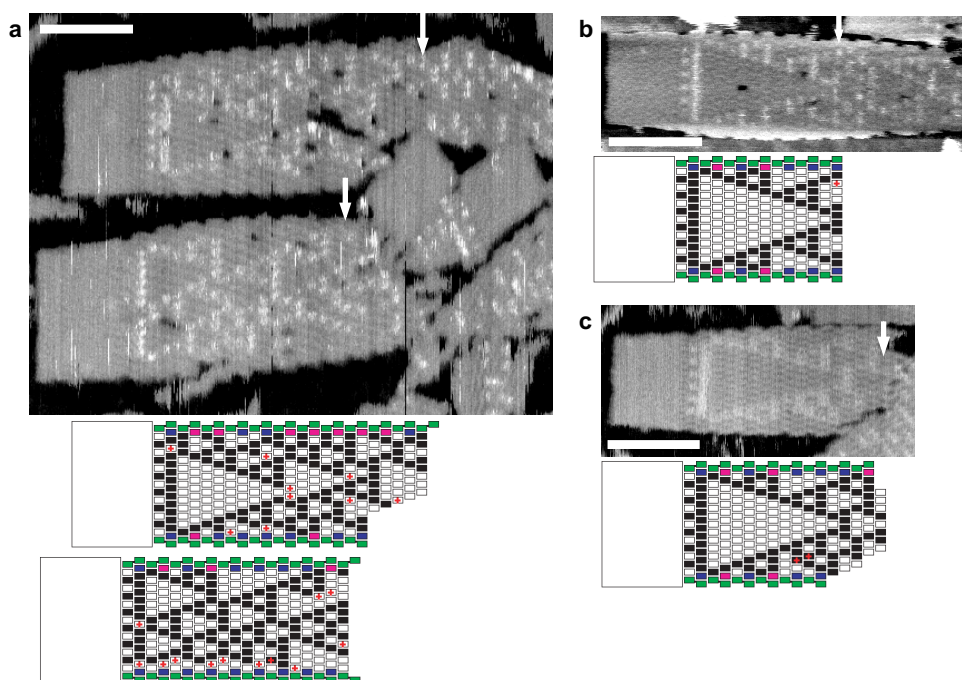


Figure S15: AFM images of four ribbons grown using all XOR tiles, and our interpretation of their tile patterns, continued from Figure S14. The interpretation of the upper crystal in image A also made use of a prior image of the same crystal, before AFM tip interactions tore out tiles near the center. [origami] = 1 nM, [each XOR tile] = 50 nM, [each boundary tile] = 10 nM. Scale bars in the images are 100 nm.

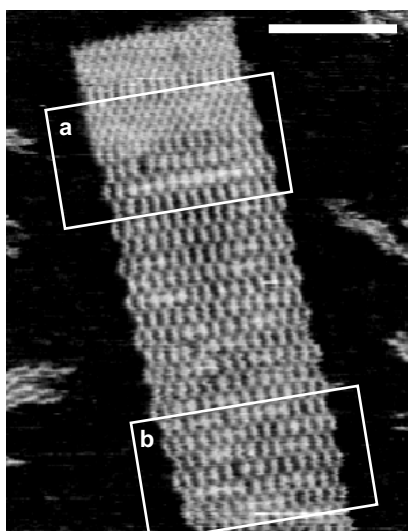


Figure S16: The AFM image of a Sierpinski ribbon with lattice defect errors in rows 1 and 18. To obtain clear images of tiles, tapping force was increased when taking this image, resulting in an inability to distinguish tiles with and without hairpins. Boxes (a) and (b) correspond with Figure 4f and g, respectively. [origami] = 1 nM, [each XOR tile] = 50 nM, [each boundary tile] = 10 nM. The scale bar is 100 nm.

References

- [1] Schulman, R. & Winfree, E. Synthesis of crystals with a programmable kinetic barrier to nucleation. *Proc. Nat. Acad. Sci. USA* **2007**, 104, 15236–15241.
- [2] Rothmund, P. W. K., Papadakis, N. & Winfree, E. Algorithmic self-assembly of DNA Sierpinski triangles. *PLoS Biol.* **2004**, 2, 2041–2053.
- [3] Barish, R. D., Rothmund, P. W. K. & Winfree, E. Two computational primitives for algorithmic self-assembly: Copying and counting. *Nano Lett.* **2005**, 5, 2586–2592.